Measurements of translational energy gain for one- and two-electron transfer in slow Ar^{q+}-He (q=15–18) collisions

H. Cederquist, C. Biedermann, and N. Selberg
Stockholm University, S-10405 Stockholm, Sweden

P. Hvelplund
Institute of Physics, University of Aarhus, DK-8000 Aarhus C, Denmark
(Received 14 July 1994; revised manuscript received 11 October 1994)

We have measured n-state-resolved energy-gain distributions for single-electron capture in Ar^{q+}-He collisions (q=15–18) at energies in the vicinity of 3.35q keV. The energy-gain scales were calibrated absolutely with precisions between a few tenths of an eV and one eV. The kinetic-energy distributions due to transfer-ionization processes (i.e., two-electron transfer followed by autoionization) were recorded and the (5,n') series appeared to be most important for Ar^{16+}. The energy-gain spectrum for true double-electron capture in Ar^{16+}-He collisions, however, indicated a dominance of strongly asymmetric (4,n') states, showing that *different* intermediate doubly excited states are dominant in the two processes.

PACS number(s): 34.70.+e, 34.50.Fa

I. INTRODUCTION

Ion-atom collisions are usually divided into the slow and the fast velocity regimes, depending on whether the projectile velocity is lower or higher than the orbital velocities of the active electrons. The main phenomenological difference between the two cases is that ionization dominates over electron capture in fast collisions, whereas the opposite relation prevails in the low velocity regime. However, not only the velocity v but also the charge state q of the projectile influences the balance between ionization and capture and a more careful identification of the relevant collision regime involves both parameters [1]. In a classical picture, the potential barrier between the projectile and the target core allows an active electron to leave the target at internuclear separations smaller than a certain critical value. If the total energy of the active electron then is negative with respect to the projectile it may be captured. The condition for this, $v < q^{1/4}\sqrt{I_1}$, where I_1 is the first ionization potential of the target, is obviously fulfilled for higher velocities when the projectile charge is high.

Moreover, it is well known that electron transfer from the target to the projectile usually is well localized to avoided crossings between quasimolecular adiabatic potential curves at the very lowest velocities ($v \ll 1$ a.u.), but that the influence from dynamic effects increases with the velocity. This was clearly demonstrated by Meyer *et al.* [2], who observed a disappearance of oscillations in the electron-capture cross section (as a function of q) for $v > 0.35$ a.u. in collisions between fully stripped ions and atomic hydrogen.

In this paper, we report measurements of n-state-resolved translational energy-gain spectra for single-electron capture in slow collisions with ions of very high charge. The partial, n-state-selective, cross sections for Ar^{q+}-He ($15 \leq q \leq 18$) collisions at $v \sim 0.058\sqrt{q}$ a.u. are in good agreement with those calculated by means of the multichannel Landau-Zener approach with the semiempirical diabatic coupling elements from Olson and Salop [3]. The energy-gain spectra for transfer ionization (i.e., two-electron transfer followed by autoionization) have been measured simultaneously for Ar^{q+}-He ($15 \leq q \leq 18$). The (n,n') series with n=5 and n' ranging from n'=6 to n'=11 appears to be preferred for q=16. The true double-electron capture spectrum for the same collision (q=16) is dominated by strongly asymmetric (4,n') states ($n' \geq 10$), which, thus, obviously have larger tendencies for radiative stabilization than the (5,n') states. Since n' apparently may be larger than the dominant principal quantum number in single-electron capture (n=7 for q=16) these results indicate that simultaneous changes of the quantum states for *two* electrons (at nearly the same value of the internuclear separation R) are as important as the processes in which the two orbitals are changed sequentially (i.e., at well separated values of R). This shows that the important quantity in the energy-resonance condition for electron transfer is the total binding energy for the two active electrons and that the binding energies for the individual electrons are not necessarily conserved [4].

In order to make correct assignments of one- and two-electron capture states, it is crucial that the energy-gain scales are calibrated absolutely with very high accuracies. The present experimental method gives a resolution of (0.3–0.4)q eV and typical energies given to the recoiling target ions are of the order of 0.1 eV. These numbers indicate the useful level of precision in the energy-gain scale and, here, we present a method which is shown to be accurate within a few tenths of an eV at collision energies above 50 keV.

The present energy-gain technique, relying mainly on high-resolution analysis of the kinetic-energy distributions of charge-reduced and decelerated projectiles, has

been used once before [5]. However, due to too low beam intensities and various other technical difficulties (such as too large instabilities in the deceleration voltage and the beam-energy defining magnetic field) the absolute energy scale had to be set by means of the classical over-the-barrier model [6,7]. A similar technique with the additional feature of coincident detection of the recoil ion charge state has been used by the group of Barat *et al.* [8] for numerous studies of collisions with projectiles of more moderate charge states (mostly $q<10$). They give an accuracy of the *relative* energy calibration of typically 1 eV, while the absolute calibration was given as (0.8–1.5)q eV [8]. They often establish the absolute energy scale by means of collisions that are regarded as well understood and arrive at absolute uncertainties of 3–5 eV. Such limitations are avoided with the present technique, since the additional free parameter in our setup, namely, the retardation voltage, can be used to determine the beam energy with very high precision.

There are only seven previous measurements of Q values for slow collisions with projectile charges $q>15$. The two earliest lead to the very important conclusion that the binding energies of captured electrons scale as $q^{1/2}$ up to very high q [9,10], but they were seriously hampered by large absolute uncertainties in ΔE (15 %) and a relatively low energy resolution ($\sim 1q$ eV). The single-electron capture and transfer-ionization processes for collisions with $q>15$ projectiles were separated clearly for the first time using translational energy-gain spectroscopy in studies of Xe^{q+}-(Ne, Ar,Xe) ($q\leq 20$) systems at 1 keV [11]. This was also achieved by Cederquist *et al.* for Xe^{q+}-Xe collisions at $4q$ keV ($q\leq 35$), which yielded the first experimental evidence for strong radiative stabilization of double Rydberg states in ions of very high charge [5]. Vancura and Kostroun [12] recently reported energy-gain measurements in the forward scattering direction for Ar^{q+}-Ar collisions for $q\leq 16$ at energies as low as $40q$ eV. This gave an absolute energy resolution ($0.5q$ eV) almost as good as the present one (0.3–0.4q eV), while the uncertainty in the energy scale was estimated to be as large as $\sim 1q$ eV. Finally, Ali *et al.* [13] and Wu *et al.* [14] extracted mean Q values for single- and multiple-electron capture by measuring the longitudinal momentum transfer to the recoiling target ions in Ar^{15+}-Ar and Ar^{16+}-He collisions, respectively.

In the following section, we will give a rather detailed account of the experimental setup and our method for absolute calibration of the energy scale. We will further discuss the expected accuracy of this method. The validity of the method, down to its claimed level of accuracy of a few tenths of an eV at about 50 keV, will be demonstrated for the dominant single-electron capture process in Ar^{16+}-He collisions. In the discussions of the results, we will report absolute n-state selective cross sections for single-electron capture. These results will be compared with calculations based on the multichannel Landau-Zener method. Finally, we will discuss two-electron transfer processes in Ar^{16+}-He collisions explicitly. There we will put the emphasis on the mechanisms for the population and the decay of intermediately formed doubly excited states.

II. EXPERIMENT

The Ar^{q+}-ion beams (q=15–18) were provided by the cryogenic electron-beam ion source ("CRYSIS") in the Manne Siegbahn Laboratory at the University of Stockholm. Singly-charged ions were first injected axially by means of an isotope separator. Then they were trapped in the source and ionized further by a 150 mA continuous electron beam with an energy of 12 keV. After reaching the desired charge-state distribution the ions were expelled in ~100 ms long pulses containing total charges of 10^{-10} to 10^{-9} C [15].

The energy and angular spreads in the beams were defined by means of a double-focusing magnet and three slits (c.f. Fig. 1). With the entrance and exit slits of the magnet (radius 0.5 m) set to 0.1 mm, the energy spread was (0.3–0.4)q eV. The third slit, mounted downstreams from the exit slit, was slightly smaller than the entrance aperture of the gas cell (ϕ=0.5 mm) and limited the angular spread to ~0.015° giving typical average count rates of 500, 300, 100, and 50 s^{-1} for q=15, 16, 17, and 18, respectively. After the gas cell, which was 10 mm long and had an exit aperture of ϕ=1 mm, the beam passed a 17 cm long field-free drift region before entering a multistage retardation lens (17 cm long) with a parabolic potential distribution. The decelerated beam then passed another field-free region (8 cm) before entering a 180° hemispherical analyzer with sphere radii r_1=142 mm and r_2=158 mm. The analyzer and the position-sensitive detector, mounted ~5 cm behind it, were held at the potential of the last stage of the retardation lens. The angular acceptance of the whole beam-energy analyzing stage was calculated to be ±0.5° when the beam energy was decreased by a factor of 20 (typical value) by means of the retardation lens. There were no entrance or exit slits for the analyzer and the energy-gain distributions were mapped directly on the detector.

We attempted to align the analyzer to the ion beam in such a way that the ions entered the analyzer field at the same potential as the last stage of the retardation lens, i.e., at the distance $r_0 = 2r_1r_2/(r_1+r_2)$ from the

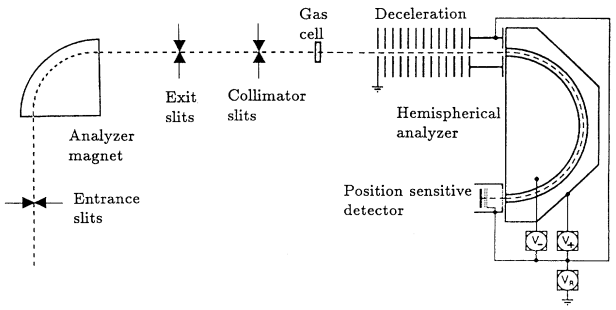

FIG. 1. A schematic of the experimental setup showing the analyzer magnet with its entrance and exit slits, the collimator slits, the gas cell, the retardation lens ("deceleration"), the electrostatic hemispherical energy analyzer, and the position sensitive detector. The power supplies for the detector and the analyzer, voltage ($\Delta V = V_+ - V_-$) are floating on the retardation voltage $V_R = V_{\rm ret}$ (c.f. text).

common center of curvature for the analyzer electrodes. Presumably this was not fully succesful and we denote the unknown errors in the angle of incidence and in the horizontal positioning of the analyzer by α and δr_0, respectively. The relation between the kinetic energy E_0, the retardation voltage $V_{\rm ret}^{\rm pri}$, and the distance r from the center of the analyzer to the point where the *primary* beam leaves the analyzer is

$$E_0 - qV_{\rm ret}^{\rm pri}(r) = qkf(r, \delta r_0, \alpha)\Delta V, \tag{1}$$

where k is a geometrical factor $k = (r_1 + r_2)/[2(r_2 - r_1)]$ and f is given by

$$f(r, \delta r_0, \alpha) = \frac{r + rr_0 \tan^2 \alpha/(r_0 + \delta r_0) + \delta r_0}{r + r_0 + \delta r_0}. \tag{2}$$

For the ions that have undergone single-electron capture (SC) to a certain n level with kinematic energy gain $\Delta E(n) \sim Q(n)$, the relation between r and the retardation voltage $V_{\rm ret} = V_{\rm ret}^{\rm SC}(r)$ is

$$E_0 - (q-1)V_{\rm ret}^{\rm SC}(r) + \Delta E(n) = (q-1)kf(r, \delta r_0, \alpha)\Delta V. \tag{3}$$

When the analyzer voltage is changed from ΔV to $\Delta V'$ (1) takes the form,

$$E_0 - qV_{\rm ret}^{\rm pri'}(r) = qkf(r, \delta r_0, \alpha)\Delta V', \tag{4}$$

where $V_{\rm ret}^{\rm pri'}(r) \neq V_{\rm ret}^{\rm pri}(r)$.

It is possible to eliminate k and $f(r, \delta r_0, \alpha)$ when δr_0 and α are the same in (1), (3), and (4) and when $r(N_{\rm pri}) = r(N_{SC}) = r(N_{\rm pri'})$ for $N_{\rm pri} = N_{SC} = N_{\rm pri'}$. Here, $N_{\rm pri}$, $N_{\rm pri'}$, and $N_{\rm SC}$ are the channel numbers (as recorded on a multichannel analyzer) for the centeroids of the two primary beams and the main peak in the single-capture spectrum, respectively. Hence, we may obtain the beam energy E_0 from (1) and (4) as

$$E_0 = q\frac{V_{\rm ret}^{\rm pri}(N) - (\Delta V/\Delta V')V_{\rm ret}^{\rm pri'}(N)}{1 - (\Delta V/\Delta V')}, \tag{5}$$

where N is the common channel number for which all three voltages are extracted. Similarly, by using (1) and (3), the energy gain $\Delta E(n)$ may be determined with high accuracy through three measurements of the retardation voltage, and two measurements of the analyzer voltage,

$$\Delta E(n) = (q-1)[V_{\rm ret}^{\rm SC}(N) - V_{\rm ret}^{\rm pri}(N)] - E_0/q. \tag{6}$$

In this way, we were able to eliminate all geometrical factors from the evaluations of ΔE and E_0.

In practice, it was not possible to set the retardation voltages for the three beams corresponding to (1), (3), and (4) with sufficient accuracies in order to get the three beams to hit the same position on the detector. In order to cope with this problem, and increase the precision in the voltages entering (5) and (6), we measured the positions on the detector (in channel numbers) as functions of the retardation voltages for the three beams.

The essence of this method is explained in Fig. 2, for one-electron transfer to the projectile in Ar^{16+}-He collisions. First, we measured the position in channels as a function of $V_{\rm ret}$ for the primary beam at ΔV=48.007 V (open circles and $V_{\rm ret}^{\rm pri}$ scale). Then, we recorded the positions of the peaks for the singly charge reduced beam (filled circles and $V_{\rm ret}^{\rm SC}$ scale) for the same value of ΔV and finally we measured the positions of the primary beam for $\Delta V'$=24.005 V (triangles and $V_{\rm ret}^{\rm pri'}$). The peak positions are determined with typical accuracies of 0.2–0.4 channels by fitting Gaussian functions to the different peaks (only data for the dominant single-capture channel is shown in the middle part of Fig. 2). The relations

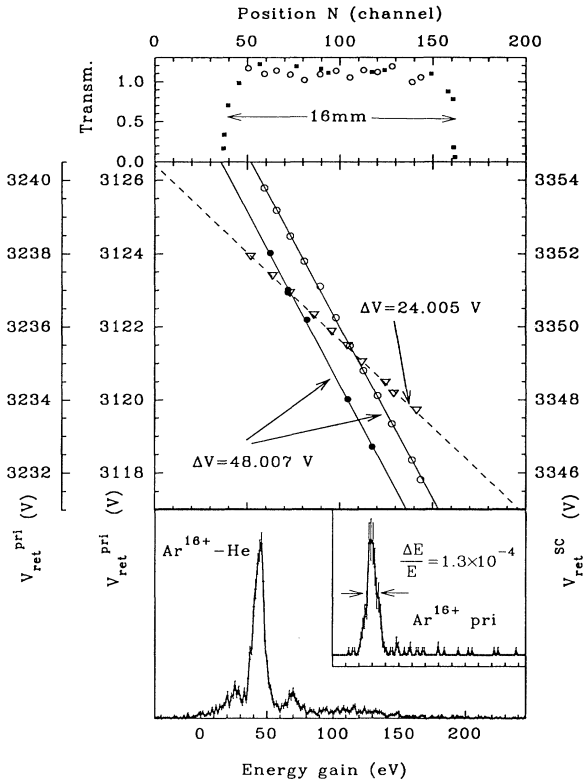

FIG. 2. The relations between the position on the detector in channels (N) and the three retardation voltages $V_{\rm ret}^{\rm pri}$ (open circles), $V_{\rm ret}^{\rm pri'}$ (triangles), and $V_{\rm ret}^{\rm SC}$ (filled circles) are shown in the middle graph. The lines are least-square fits to these three sets of data under the condition that the two lines with the same ΔV (=48.007 V) should have the same slope. The upper part of the figure shows relative transmission probabilities (including detection efficiency) as a function of N for the $V_{\rm ret}^{\rm pri}$ data set and an independent set of data (filled squares) extending all the way out to the walls of the analyzer (the analyzer gap is 16 mm and full transmission is obtained within a ~11 mm wide central region). When the parameters of the three lines in the middle graph have been determined, any channel can be used to determine the ΔE value corresponding to the peak following the $V_{\rm ret}^{\rm SC}(N)$ line. The relative energy calibration is then given by the common slopes of the two parallell lines. The shape of the primary Ar^{16+} beam is shown as an inset in the lower figure, which displays one of the single-capture spectra (including also transfer-ionization processes).

between peak positions and retardation voltages are linear with reasonably high accuracies (c.f. below) within a ~11 mm wide central region on the detector. Once the three lines of Fig. 2 are established, it becomes possible to determine ΔE for an arbitrarily chosen channel number N by extracting the three voltages $V_{\rm ret}^{\rm pri}(N)$, $V_{\rm ret}^{\rm SC}(N)$, and $V_{\rm ret}^{\rm pri'}(N)$ and enter them in (5) and (6). The energy-gain scale relative to the position of the dominant peak is given by the common slope of the two ΔV=48.007 lines, which was measured to be -1.4050 ± 0.0075 eV/ch.

The main contributors to the uncertainty in ΔE are: The limited accuracies in the measurements of $V_{\rm ret}$ and ΔV; The limitations in the determinations of peak positions and the imaging quality of the detector; The deviations from true linear relations between $V_{\rm ret}$ and N; Drifts in the field of the bending magnet, and the retardation and analyzer voltages. The voltages $V_{\rm ret}^{\rm pri}$, $V_{\rm ret}^{\rm pri'}$, and $V_{\rm ret}^{\rm SC}$ for individual data points are measured with a resolution of 10 mV, which result in typical uncertainties of ~5 mV in the values $V_{\rm ret}^{\rm pri}(N)$, $V_{\rm ret}^{\rm SC}(N)$, and $V_{\rm ret}^{\rm pri'}(N)$ extracted from the three lines of Fig. 2. This number includes uncertainties in the peak positions and the imaging quality of the detector. The analyzer voltages are measured with a resolution of 1 mV and, assuming for a moment that the nonlinearities and the drifts mentioned above do not contribute, we arrive at an error in ΔE of only 0.1 eV. The drifts in the retardation and analyzer voltages were found to be smaller than 10 mV and 1 mV during the measurements, respectively, while the magnetic field mostly was stable within 1 m Gauss. We estimate that the two former errors together may contribute at the level of 0.1 eV, while the latter one gives 0.3 eV.

We wish to stress that the expressions (5) and (6) for ΔE and E_0 are valid also when the full (nonlinear) expressions for $V_{\rm ret}(r)$ are used and that the errors introduced by using linear relations between $V_{\rm ret}$ and N are small. In order to discuss the latter point, we assume for a moment that α=0 and δr_0=0. The expression for the primary beam (1) can then be written:

$$E_0 - qV_{\rm ret}^{\rm pri} = q\frac{k}{2}\frac{1+(\delta r/r_0)}{1+(\delta r/(2r_0))}\Delta V \approx q\frac{k}{2}\left[1+\frac{\delta r}{2r_0}-\left(\frac{\delta r}{2r_0}\right)^2+\cdots\right]\Delta V\ , \qquad (7)$$

where δr is the deviation in the beam-exiting position from that of the circular trajectory with radius r_0. Analogous expansions can be made for (3) and (4). For δr=2 mm the quadratic term amounts to 0.7 % of the linear one or a deviation of 0.01 V in the retardation voltage at ΔV=48 V. Moreover, since the true $V_{\rm ret}^{\rm pri}(N)$ and $V_{\rm ret}^{\rm SC}(N)$ curves have the same functional form and since the deviation from the line scales linearly with $\Delta V'/\Delta V$, this type of error would cancel perfectly in the evaluations of E_0 and ΔE if the data points would be recorded for the same set of channels in all three measurements [c.f. (5) and (6)]. Since this condition is not fulfilled for the case shown here, we estimate that there is a small error emanating from this effect (<0.01 V) and that all the errors discussed so far amount to a total uncertainty of ±0.3 eV.

The method described above relies on the assumption that the three voltages extracted for a given (fixed) channel number can be associated with identical trajectories. That is, δr_0 and α must be unchanged during the three series of measurements. This requirement appears to be easy to meet for the primary and charge-reduced beams (at the same value of ΔV) since their charge-to-energy ratios, and hence their sensitivities to stray fields, are the same after the deceleration. This is not the case for measurements at different settings of the analyzer voltage. We made an independent experimental test of this point by measuring the energy of the primary beam with the present method for several pairs of analyzer voltages. Since the result (after a drastic reduction of the stray magnetic field by means of μ-metal shields) was stable down to at least ΔV=20 V, we concluded that the influence from this source of error was small.

The relations between the intensities in different spectra, as, for example, the ones for true double-electron capture and transfer ionization, were determined by normalizing to the accumulated charge collected on the exit slit for the analyzing magnet. This method can be used to determine absolute charge-exchange cross sections, but it has a clear drawback since it relies on a constant relation between the number of ions not passing the exit slits and the number of ions passing the gas cell, which is situated ~2 m downstreams. From the scatter of absolute cross sections obtained for five different runs with Ar^{16+}-He collisions, we concluded that the normalization can be trusted to within ±25%.

III. RESULTS AND DISCUSSION

A. Single-electron capture

1. Q values

The present energy calibration yielded the result ΔE=47.1±0.3 eV for the main peak in the singly-charge-reduced energy-gain spectrum of Ar^{16+}-He collisions, while E_0/q was 3349.3±0.1 V. The kinematic energy shift $Q-\Delta E$ is estimated to be 0.2 eV using the formula given by, e.g., Nielsen *et al.* [17] and assuming that the projectile is scattered by an angle $\theta=Q/(2E_0)$. The resulting Q value of 47.3±0.3 eV appears to indicate that the lower l states in the n=7 manifold are dominant since the calculated Q values (Hartree-Fock) range from 47.6 eV ($7s$) to 46.5 eV ($7i$). All the present results for single-electron capture are summarized in Fig. 3. In Table I, we compare the experimental Q values (including the estimated kinematic energy shifts) with theoretical Q values based on single-configuration Hartree-Fock values for the binding energies. The energy-gain scales for Ar^{15+} and Ar^{17+} are obtained with the method described for Ar^{16+}. The calibration for Ar^{18+} relies on much fewer data points and

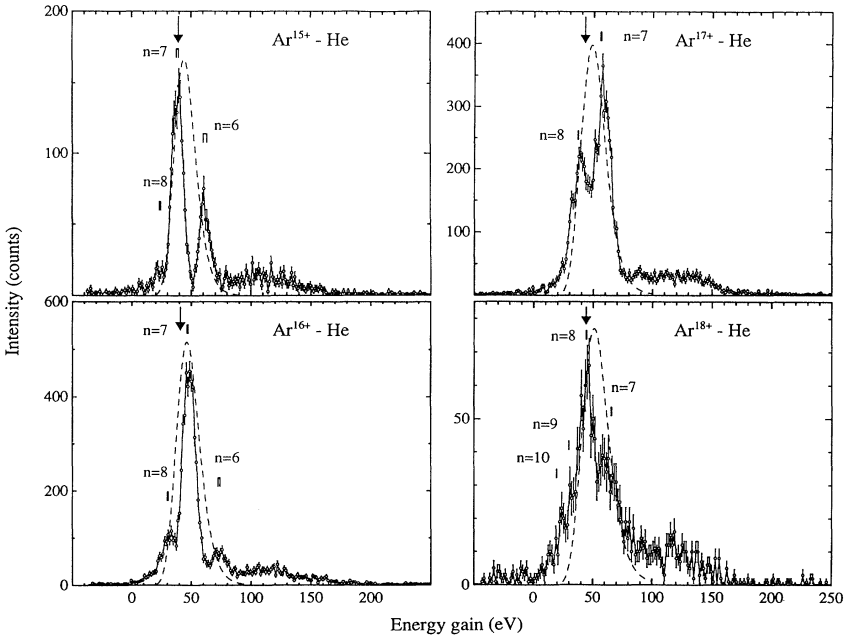

FIG. 3. The energy-gain spectra of single-electron capture and transfer ionization for Ar^{15+} (upper left), Ar^{16+} (lower left), Ar^{17+} (upper right) and Ar^{18+} (lower right) colliding on He at energies in the vicinities of $3.35q$ keV. The predictions for single-electron capture from the extended classical over-the-barrier model are indicated by arrows, while the theoretical Q values deduced from single-configuration Hartree-Fock calculations are shown as brackets (when the energy splittings between l states are non-negligible). The reaction windows, i.e., the Landau-Zener cross section for a hypothetical two-level system using the Olson-Salop coupling are indicated with dashed lines (in arbitrary intensity scales with respect to the measured distributions). The beam-defining slits were set to 0.1 mm for the three lower charge states while they were 0.2 mm for q=18.

the determination of the channel number $N=N(r=r_0)$, corresponding to the circular trajectory $r=r_0$. The agreement between the actually realized positions in ΔE and those expected from the Hartree-Fock calculations is quite satisfactory. The predictions for the Q values from the extended classical over-the-barrier (ECB) model [7] are indicated by arrows in Fig. 3 and for Ar^{15+}, Ar^{16+}, and Ar^{18+}, they are very close to the dominant peaks n=7, n=7, and n=8, respectively. We estimate typical scattering angles for single-electron capture to be ~0.03°, which lies well inside the angular acceptance of the apparatus (0.5°).

Ali *et al.* [13] give an uncertainty in their absolute energy scale of about 4 eV for 50 keV Ar^{15+}-Ar collisions, while Wu *et al.* [14] (using the same experimental setup) give a mean Q value of 32±1 eV (extracted from a figure) for single-electron capture in Ar^{16+}-He collisions at similar energies. Based on this finding they reported a dominance of capture to n=8 in Ar^{16+}-He collisions [14], while we find a strong dominance of capture to n=7 at Q=47.3±0.3 eV at nearly the same collision energy. In addition, we measure the Q values of two much smaller side peaks to be 30.3±1.4 eV and 70.6±1.4 eV, which are in agreement with the expected positions for capture to the n=8 and n=6 levels, respectively. This agreement suggests very strongly that the present result is correct.

2. *Cross sections*

For the four specific cases investigated here one or two n states are strongly populated in single-electron capture. The total absolute cross section for net one-electron transfer to the projectile in Ar^{16+}-He collisions at $3.35q$ keV was measured to be $(52\pm13)\times10^{-16}$ cm^2, which is consistent with the result of Vancura *et al.* of $(50.4\pm7.3)\times10^{-16}$ cm^2 at $2.3q$ keV [16]. Once the absolute cross-section scale is defined, the present technique obviously allows us to determine state-selective cross sections for single-electron capture (c.f. Table I) and total cross sections for transfer ionization. The absolute cross sections have been measured directly as described in the preceding section for q=16 and q=17, while the absolute scale for q=15 was set by means of the result of Vancura *et al.* [16]. The current on the magnet exit slits was too low for a reliable normalization for q=18 and, therefore, only relative cross sections may be deduced in that case. It should be noted here that we have not tried to correct the cross section for possible blends by close-lying transfer ionization channels. However, we expect that the influence from such corrections are rather small (c.f. the discussion of two-electron processes in Ar^{16+}-He in the next section).

The experimental cross sections are compared with the corresponding quantities calculated within the multichannel-Landau-Zener (MCLZ) approach [18,19] using the semiempirical diabatic coupling elements of Olson and Salop [3] *without* any reduction factor [19,20]. The quantitative comparisons are shown in the Table I, while qualitative comparisons are offered in the forms of reaction windows (dashed curves) in Fig. 3. The experimental and theoretical results agree for q=15 and q=16, while the absolute levels of the experimental cross sections for q=17 lie 50% above the theoretical ones. The distribution of the total single-electron capture cross section on different n states is, however, reproduced by the calculations in all cases. These observations strongly suggest that it is correct to use the original semiempirical formula by Olson and Salop. This is also quite reasonable, since the rather highly excited single-capture states populated in the present collisions closely resemble truly hydrogenic states and energy separations between neighboring l levels are much smaller than typical adiabatic energy splittings. Obviously, the correction factor introduced by Taulbjerg [20] for the case of open-core projectiles with *large* separations between the different l levels of n manifolds should not be applicable here, in accordance with our experimental results. For the present collisions, it is further incorrect to view all the valence electrons of multiple-electron targets (like He) as equivalent and to increase the effective coupling strength with the number of such electrons [18,19]. Instead, it appears that the target should be viewed as a one-electron target (where the electron is bound by the first ionization potential) in order to describe single-electron capture.

TABLE I. Theoretical (Q^{HF}) and experimental Q values (Q^{expt}; i.e., the sum of the experimental ΔE value and the estimated kinematic energy shift) for single-electron capture in Ar^{q+}-He collisions ($15 \leq q \leq 18$). The table also shows absolute experimental (σ_{expt}) and theoretical (σ_{OS}) state-selective cross sections for q=15-17. The latter are calculated by means of the multichannel Landau-Zener method (MCLZ) with the coupling element given by Olson and Salop (OS). The absolute experimental cross-section scale for Ar^{15+}-He is normalized to the results of Ref. [16].

Process	(eV)	Q^{expt} (eV)	Q^{HF}	σ_{expt} (10^{-16} cm^2)	σ_{OS} (10^{-16} cm^2)
		Ar^{15+}-He			
$n=7$	38.5 ± 0.4	$37.9 \leftrightarrow 39.7$	27.6		5.5±23.4
$n=6$	61.7 ± 0.4	$60.5 \leftrightarrow 63.4$	11.3		2.3±8.8
TI			9.7		1.9±
		Ar^{16+}-He			
$n=8$	30.3 ± 1.4	$29.9 \leftrightarrow 30.6$	5.6		1.1±5.6
$n=7$	47.3 ± 0.3	$46.5 \leftrightarrow 47.6$	29		5.8±27.6
$n=6$	70.6 ± 1.4	$72.2 \leftrightarrow 73.9$	4.4		0.9±4.6
TI			13		2.6±
DC			1.5		0.7±
		Ar^{17+}-He			
$n=8$	37.0 ± 1.0	$37.3 \leftrightarrow 36.9$	22.0		4.4±15.0
$n=7$	56.8 ± 1.0	$56.3 \leftrightarrow 55.6$	36.0		7.2±23.7
TI			10.4		2.1±
		Ar^{18+}-He			
$n=8$	42.8 ± 1.5	44.3			
$n=7$	65.3 ± 1.5	65.4			

Meyer *et al.* [2] found that the oscillations in single-capture cross sections (as a function of q), observed at low velocities, become less pronounced already in the $v \sim 0.1$ a.u. region. They interpreted this disappearance of an oscillatory behavior as due to an increasing importance of nonlocalized electron transitions and they further concluded that the assumptions on which the Landau-Zener model is based become invalid at velocities much above 0.3 a.u. The present good agreement between state-selective model and experimetal cross sections strongly suggest that the assumptions of the Landau-Zener model holds for Ar^{q+}-He collisions at $v \sim 0.2$ a.u. when q=15, 16, 17, and 18.

B. Transfer ionization and true double-electron capture

Our measured total cross sections for single-electron capture are roughly 10–20 % lower than the cross sections predicted by the ECB model. The experimental cross sections for the dominant two-electron process (transfer ionization) are considerably lower than the model cross sections for two-electron removal from the target. The latter feature has been observed before as anomalously low ratios (in relation to the ECB predictions) between two- and one-electron removal from the target in Xe^{q+}-He collisions up to q=44 [21].

It is generally accepted that the transfer-ionization and true double-electron-capture processes in slow ion-atom collisions involving highly charged ions proceed via the formation of intermediate doubly excited states. In the following section, we will discuss whether these states are the same for both processes or if there is a difference in the types of states leading to the two reactions. We have chosen to limit this discussion to the Ar^{16+}-He case.

1. Q values

In Fig. 4, we show energy-gain spectra for single-electron capture (top), transfer ionization (middle), and true double-electron capture (DC) (bottom) for Ar^{16+}-He collisions. We note that the weak structure in the transfer-ionization spectrum would be consistent with population of the doubly excited (5,n') states with n' ranging between n'=6 and n'=11. However, at this point we refrain from making a definite assignment of the ob-

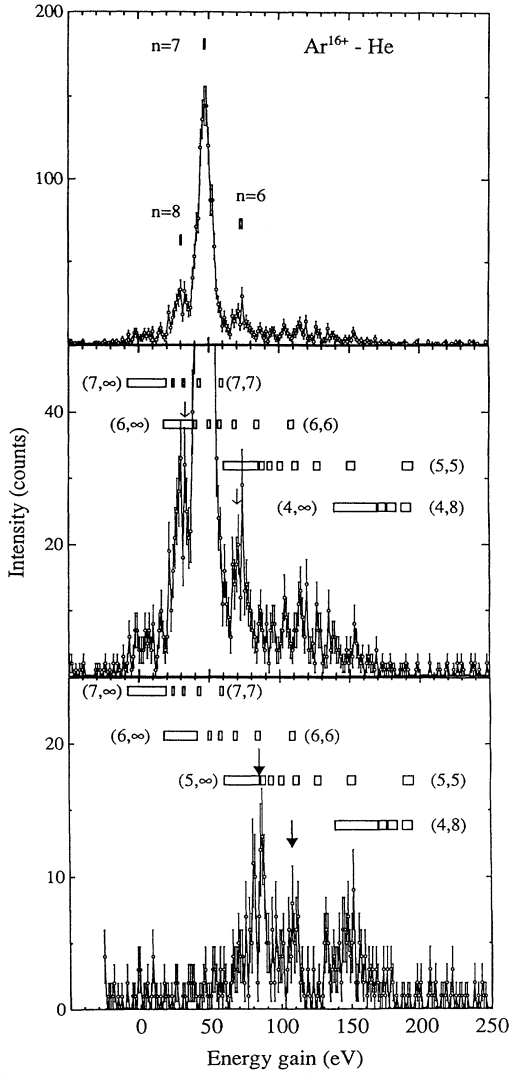

FIG. 4. Energy-gain spectra for single-electron capture (top), transfer ionization (middle), and true double-electron capture (bottom) in Ar^{16+}-He collisions. The middle spectrum is identical to the top spectrum, but it is shown with a different vertical scale. The single-configuration Hartree-Fock energies of the (4,n'), the (5,n'), the (6,n'), and the (7,n') series are shown in the two lower figures, The widths of individual boxes for the lower (n, n')-states reflect the energy spreads of states with different angular momenta within certain (n, n') manifolds. The n' quantum numbers of the states in the boxes furthest to the right in each series are indicated to right and the following boxes (going to the left) represent states for the following (higher) values of n'. The labels for the states with the lowest possible Q values within a given series are shown to the left [(7,∞), (6,∞), etc.]. The expected positions of the three dominant single-electron channels are indicated in the upper figure. The two thin arrows in the middle figure show the positions where transfer-ionization satellites (to the n=6 and n=8 single-capture peaks) could appear. The two bold arrows in the lower figure indicate the expected positions of the double-collision peaks at Q=87 and 109 eV (c.f. text). Note that the intensity in the true double-capture spectrum (bottom) cannot be directly related to the intensity in the transfer-ionization spectrum (middle) due to differences in the data-taking times.

served features. The main reasons for this is the low statistical level of the data and the fact that the peaks probably are too narrow in realtion to what one would expect from the broadening due to electron emission from the projectile.

A part of the double-capture spectrum (bottom Fig. 4) is contaminated by double collisions, but this contribution may be estimated since the Q-value distributions for single-electron capture in Ar^{16+}-He and Ar^{15+}-He are known (from the present experiment) and the corresponding absolute cross sections can be deduced from the present study and Vancura *et al.* [16]: We estimate the l-averaged lifetime of the n=7 state in Ar^{16+} to be $\sim 10^{-11}$ s, which is much shorter than the time it takes for the ions to pass the gas cell (~20 ns). This means that the probability for creating *doubly excited* states through collisions with *two different* target atoms is expected to be very small and instead the most likely product of a double collision event is the creation of a singly excited projectile state (there is time for the excitation resulting from the first collision to relax before the second collision occurs). The double collisions will thus appear in the energy-gain spectrum for projectiles which have picked up two electrons. The dominant *apparent* Q values for these events are ~86 (47.1+38.5, c.f. Fig. 3) and ~109 (47.1+61.7) eV. The two peaks to the left in the lower spectrum of Fig. 4 fit these values on an absolute scale. Further, using the normalization of the intensities of the spectra, which was described in the experimental section, we find that the measured peak intensities may be fully accounted for by such false events. Moreover, the intensity relation between the two double-collision peaks (indicated by arrows in the lower part of Fig. 4) is the same as the relation between the two dominant peaks in Ar^{15+}-He collisions (c.f. Fig. 3). We thus conclude that the true double-electron capture process is dominated by the intermediate population of $Ar^{14+}(4,n')$ states.

From Figs. 3 and 4 it is evident that the cross sections for transfer ionization (the structures to the right of the peaks due to single-electron capture) are substantially smaller than the corresponding ones for single-electron capture. For the Ar^{16+}-He collisions, we measure $\sigma_{TI}(Q_{TI} > 80)/\sigma_{SC}$=0.13±0.2 (1.3 keV/u) which is much lower than the result of Wu *et al.* [14], who report σ_{TI}/σ_{SC}=0.24 at ~0.9 keV/u and a rather strongly increasing trend for increasing velocities. Wu *et al.* give an average Q value for transfer ionization of 94±3 eV, while we deduce Q_{mean}=111±2 eV from our distribution *above* Q=80 eV. We estimate typical projectile scattering angles to be around 0.1-0.15° for the various two-electron transfer processes of interest here. This well within the angular acceptance of the apparatus (±0.5°).

The present low cross-section ratio and high Q_{mean} value for transfer ionization may be qualitatively accounted for by observing that there are satellite peaks close to the n=6 and n=8 single-capture peaks, which we tentatively ascribe to doubly excited (6,8) and (7,9) states, respectively (c.f. the arrows in the middle part of Fig. 4). It is clear that the statistical significance of these satellites is not very high based solely on the data in Fig. 4. However, the "doubleness" of the n=8 and

n=6 single-capture peaks appeared in essentially all of the many spectra which we recorded under various experimental conditions and it is for this reason that we believe that they are real. We consider it to be rather likely that the population mechanisms for the transfer-ionization processes below Q=80 eV are different from the ones where the inner electron is in a n=4 or n=5 state and a reasonable, albeit very tentative, explanation is that rotational couplings play an important role. This idea stems from the fact that some doubly excited states, built on inner electrons in $n>5$, are close to degenerate (at infinite R) with the dominant single-capture channels in a fashion closely resembling the situation recently discussed for true double-electron capture in slow C^{4+}-Ne collisions [22]. Quite possibly several more members of the (6,n') and the (7,n') states are populated, but they are too close to the strong n=7 single-capture peak to be visible in Fig. 4. Due to these difficulties, we refrain from trying to extract definite numbers for the mean Q value and the cross section ratio. It is clear, however, that the inclusion of the satellites would bring both values closer to the results of Wu *et al.* [14].

It is much easier to derive a mean Q value for true double-electron capture and we arrive at Q_{mean}=143.3±3 eV. This is in strong disagreement with the results of Wu *et al.* who report the same value as for transfer ionization (94±3 eV). Thus, as opposed to Wu *et al.* [14], the present results clearly shows that *different* intermediate doubly excited states are responsible for the transfer ionization (5,n') and true double-electron-capture processes (4,n').

2. *Radiative stabilization and autoionization*

We extract an average probability for radiative stabilization of 9%, which is consistent with the results of Wu *et al.* [14]. From the present data, it further appears that the probabilities for radiative stabilization, $P_{\text{rad}}(n,n')$, are close to zero for the (5,n') states with $n'>6$, while the (4,n') states below the $Ar^{15+}(4s)$ limit mostly stabilize radiatively. This result demonstrates that a state with an initial high degree of asymmetry $n \ll n'$ [like the present (4,n') states centered on n'=15] in general will be more likely to keep both electrons than a quasisymmetric $n \approx n'$ or symmetric $n = n'$ one [like the present (5,n')-states centered on n'=8]. Some of the initially populated states reside fairly high above the nearest lower ionization limit, which according to Hansen [23] (who has calculated the branching ratios for doubly excited Ar^{14+} states lying slightly higher than the ones we observed) will make autoionization less probable than otherwise. As mentioned above, this condition is not fulfilled for the (4,n') states *above* the 4s limit and, therefore, they mostly appear in the transfer-ionization spectrum (c.f. Figs. 5 and 6).

In Fig. 5, we show our calculated single-configuration Hartree-Fock energies for the doubly excited Ar^{14+} states of immediate interest. Isotropic autoionization of (5,8) and higher (5,n') towards the n=4 limits would lead to substantial broadening of the lines, while such emission from some (5,7) and possibly some of the (5,6) states mixed with (4,n') states would give less broadening.

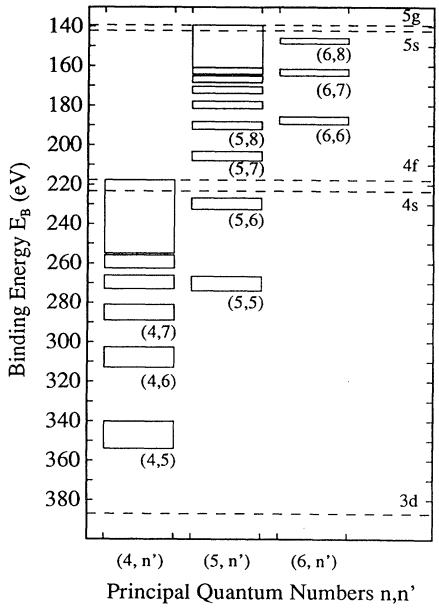

FIG. 5. Single-configuration Hartree-Fock binding energies for some singly excited $Ar^{15+}(nl)$ states (dashed lines) and doubly excited $Ar^{14+}(n,n')$ states.

3. *Population mechanisms*

The population of the n=4 and the n=5 shells in two-electron transfer is quite reasonable in view of the ECB model which predicts n=4.8 for the inner electron. However, the present experimental results show that the n' state of the outer electron in two-electron transfer, easily may be much higher than the dominant n state for single-electron capture (n=7 for Ar^{16+}-He). This has been observed before, but only for collisions involving ions of much lower charge states. Even though we cannot draw definite conclusions about the dominant reaction mechanisms from the energy-gain spectra alone, the specific energy-level structure of the Ar^{16+}-He system leads to the following observations for the population of the (5,n') series: The crossing between the incident channel and the n=6 single-capture channel is strongly adiabatic and, therefore, one may expect the two dominant paths to the (5,n') states to proceed via the incident channel, and the n=6 or n=7 single-capture channels (c.f. Fig. 6). If we for a moment *assume* that the electrons are transferred sequentially and that the second electron only may leave the target when the potential barrier is sufficiently low, it is clear that only the (5,6) states may be populated from the n=6 channel and only the (5,6), (5,7), and the (5,8) states may be populated from the n=7 channel. However, in a more realistic picture of charge-transfer built on the Landau-Zener model and the reaction-window concept there can be nonvanishing probabilities for electron transfer at internuclear separations larger than the limiting ones set by the ECB model. This means that transitions from the n=7 channel to higher

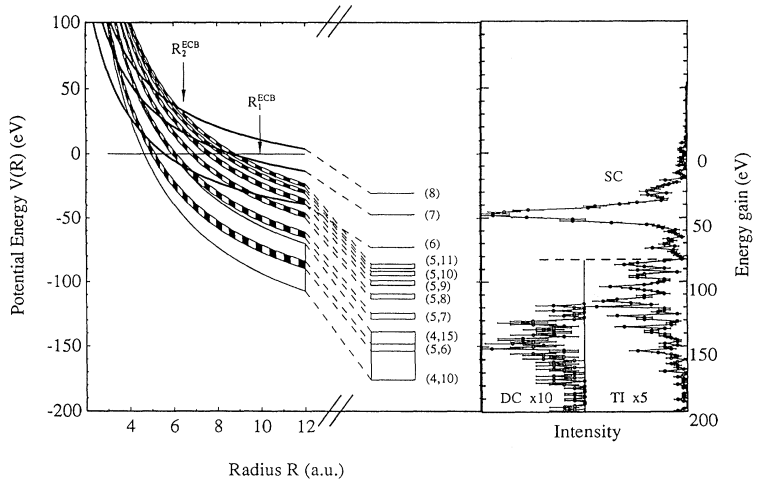

FIG. 6. A schematic of the quasimolecular potential energy diagram of Ar^{16+}-He. The incident channel is flat and the single-capture channels only contain the Coloumbic term. The potential curves for two-electron transfer contain the $2(q\text{-}2)/R$ term [the $(5,n')$ series] or the $2(q-1)/R$ term for highly asymmetric $(4,n')$ states. The limits for transfer of "the first" and "the second" electron according to the ECB model are indicated by R_1^{ECB} and R_2^{ECB}, respectively. The measured Q-value distributions for single-electron capture (SC), transfer ionization (TI), and true double-electron capture (DC) are shown at the right part of the figure. The latter two are magnified by factors of 5 and 10, respectively.

members of the $(5,n')$ series cannot be excluded although they cross outside the limit R_2^{ECB} set by the ECB model (c.f. Fig. 6).

Regardless of which one of these mechanisms dominates, it appears that two orbitals have to change simultaneously (i.e., at nearly the same value of R) when states above the (5,7) states are populated. This conclusion would obviously also hold in the case that the two-electron transfer channels are populated directly from the incident channel. The efficiencies of electron transfer at avoided crossings of adiabatic potential curves are, thus, rather insensitive to wether the transition would lead to drastic changes of one-electron binding energies or not as long as the sum of the binding energies for the two electrons does not change.

The population mechanism for the $(4,n')$ channels must be discussed in the context of possible mixings with more symmetric states. There are only two groups of states that are close to this series at infinite internuclear separations. These are the (5,5) and the (5,6) states, which lie in the vicinities of the (4,8) and (4,15) states, respectively. It is very important to note that the path directly from the incident channel to the $(4,n')$ channels is virtually closed by the strong adiabaticity of the n=6 single-capture channel. It is, thus, tempting to conclude that only sequential transfer via one or several of the three active single-capture channels are possible.

It further seems that the population of the $(4,n')$ series might have large similarities to the population of strongly asymmetric states in two-electron transfer observed by Gaboriaud *et al.* for N^{7+}-Kr collisions [24]. In *that* case (there are several more reported in the literature. See, e.g., [25]) it was argued that an R-dependent mixing between the (4,4) and the $(3,n')$ series was responsible for the population of the latter one and, further, that this explained the surprisingly large degree of radiative stabilization at such a relatively low q. This process was named "auto transfer to Rydberg states" and relies on the better screening of the projectile core charge by more symmetric doubly excited states close to the crossing region of interest. The potential curve structure of the present Ar^{16+}-He collisions (c.f. Fig. 6) show substantial similarities to the N^{7+}-Kr system in that it has quasi-symmetric (5,6) states imbedded in the asymmetric series $(4,n')$ at infinite values of R. Thus, two possible collision mechanisms that may lead to population of the highly asymmetric $(4,n')$ series proceed through one or several of the active single-capture channels and to $(4,n')$ states either via the (5,6) states or directly. Again, there is no way to distinguish between these possibilities by means of the energy-gain spectra alone. However, regardless of which one of the mechanisms that is most important, the last steps involve changes of the principal quantum numbers for both the active electrons.

IV. CONCLUSION

In this paper, we have reported experimental results on state-selective single-electron capture in slow collisions between Ar ions of the four highest charge states and He. For these measurements, we used method which made it possible to calibrate the energy-gain scales with high accuracies, as demonstrated in detail for Ar^{16+}-He collisions. The comparison between measured and calculated state-selective cross sections for single-electron capture strongly indicates that the correct values of the diabatic

coupling strengths are given by the semiempirical formula derived by Olson and Salop. As discussed above, it is hardly surprising that this applies to the strongly hydrogenlike levels, populated in Ar^{q+}-He collisions (q=15–18), since the formula was derived for bare nuclei colliding with atomic hydrogen. While the larger ionization potential of the He target has to be taken into account, we find that no correction for the number of available valence electrons is necessary in the present case. The rather close agreement between the present experimental and theoretical results on single-electron capture lead to the conclusion that electron transfer is well localized to avoided crossings of adiabatic potential curves.

The analysis of transfer ionization processes has been concentrated to the Ar^{16+}-He case. These results indicate that processes which require *simultaneous* changes of the principal quantum numbers for two electrons may be as important as those in which the two orbitals are changed *sequentially*. We have further reported the corresponding energy-gain spectrum for true double-electron capture, which clearly shows a different Q-value distribution as compared to that of transfer ionization. Our results suggests strongly that fairly symmetric $(5,n')$ states are dominant in transfer ionization, while strongly asymmetric $(4,n')$ states lead to true double-electron capture.

ACKNOWLEDGMENTS

This work was supported by the Swedish Natural Science Research Council (NFR) and the Carlsberg foundation in Denmark. We are grateful to Anders Bárány for reading the manuscript carefully.

[1] N. Bohr and J. Lindhard, K. Dan. Vidensk. Selsk. Mat. Fys. Medd. **28**, 7 (1954).
[2] F. Meyer, A.M. Howald, C.C. Havener, and R.A. Phaneuf, Phys. Rev. Lett. **54**, 2663 (1985).
[3] R.E. Olson and A. Salop, Phys. Rev. A **14**, 579 (1976).
[4] N. Stolterfoht, C.C. Havener, R.A. Phaneuf, I.K. Swenson, S.M. Shafroth, and F.W. Meyer, Phys. Rev. Lett. **29**, 96 (1986).
[5] H. Cederquist, H. Andersson, G. Astner, P. Hvelplund, and J.O.P. Pedersen, Phys. Rev. Lett. **62**, 1465 (1989).
[6] H. Ryufuku, K. Sasaki, and T. Watanabe, Phys. Rev. A, **21**, 745 (1980).
[7] A. Bárány, G. Astner, H. Cederquist, H. Danared, S. Huldt, P. Hvelplund, A. Johnson, H. Knudsen, L. Liljeby, and K.G. Rensfelt, Nucl. Instrum. Methods Phys. Res. Sect. B **9**, 397 (1985).
[8] M. Barat, M.N. Gaboriaud, L. Guillemot, P. Roncin, H. Laurent, and S. Andriamonje, J. Phys. B **20**, 5771 (1987).
[9] T. Iwai, Y. Kaneko, M. Kimura, N. Kobayashi, A. Matsumoto, S. Ohtani, K. Okuno, S. Takagi, H. Tawara, and S. Tsurubuchi, J. Phys. B **17**, L95 (1984).
[10] H. Tawara, T. Iwai, Y. Kaneko, M. Kimura, N. Kobayashi, A. Matsumoto, S. Ohtani, K. Okuno, S. Takagi, and S. Tsurubushi, J. Phys. B **18**, 337 (1985).
[11] P. Hvelplund, A. Bárány, H. Cederquist, and J.O.K. Pedersen, J. Phys. B **20**, 2515 (1987).
[12] J. Vancura and V.O. Kostroun, in *Proceedings of the VIth International Conference on the Physics of Highly Charged Ions, Manhattan, Kansas 1992,* edited by P. Richard, M. Stöckli, C.L. Cocke, and C.D. Lin, AIP Conf. Proc. No. 274 (AIP, New York, 1993).
[13] R. Ali, C.L. Cocke, M. Stöckli, S. Cheng, and M.L.A. Raphaelian, Phys. Rev. Lett. **69**, 2491 (1992).
[14] W. Wu, J.P. Giese, I. Ben-Itzhak, C.L. Cocke, P. Richard, M. Stöckli, R. Ali, H. Schöne, and R.E. Olson, Phys. Rev. A **48**, 3617 (1993).
[15] E. Beebe, L. Liljeby, A. Pikin, M. Björkhage, Å. Engström, and A. Pääl, Nucl. Instrum. Methods Phys. Res. Sect. B (to be published).
[16] J. Vancura, V.J. Marchetti, J.J. Perotti, and V.O. Kostroun, Phys. Rev. A **47**, 3758 (1993).
[17] E.H. Nielsen, L.H. Andersen, A. Bárány, H. Cederquist, J. Heinemeier, P. Hvelplund, H. Knudsen, K.B. MacAdam, and J. Sorensen, J. Phys. B **18**, 1789 (1985).
[18] L.R. Andersson, J.O.P. Pedersen, A. Bárány, J.P. Bansgaard, and P. Hvelplund, J. Phys. B **22**, 1603 (1989).
[19] C. Biedermann, H. Cederquist, L.R. Andersson, J.C. Levin, R.T. Short, S.B. Elston, J.P. Gibbons, H. Andersson, L. Liljeby, and I.A. Sellin, Phys. Rev. A **41**, 5889 (1990).
[20] K. Taulbjerg, J. Phys. B **19**, L367 (1986).
[21] H. Cederquist, E. Beebe, C. Biedermann, Å. Engström, H. Gao, R. Hutton, J.C. Levin, L. Liljeby, T. Quinteros, N. Selberg, and P. Sigray, J. Phys. B **25**, L69 (1992).
[22] N. Keller, R.D. Miller, M. Westerlind, S.B. Elston, I.A. Sellin, L.R. Andersson, C. Biedermann, and H. Cederquist, Phys. Rev. A **50**, 462 (1994).
[23] J.E. Hansen, J. Phys. (Paris) Colloq. C1-603 (1989).
[24] M.N. Gaboriaud, P. Roncin, and M. Barat, J. Phys. B **26**, L303 (1993).
[25] M. Barat and P. Roncin, J. Phys. B **25**, 2205 (1992).